JOURNAL OF MATERIALS SCIENCE 20 (1985) 4399–4406

Partition of deformation and anelastic energies in multiple impacts in copper

IRWIN G. GREENFIELD, ELSA B. ITURBE
College of Engineering, University of Delaware, Newark, Delaware 19716, USA

Response of a copper specimen to a large number of impacts by a single indenter was investigated. Work hardening produced during the first few impacts was studied based on measurements of impact parameters. Analysis of the energy distribution during impacts indicated that a large portion of the energy is expended in anelastic effects. Study of the subsurface microstructure showed a dislocation cell structure similar to the cell structure developed in fatigued materials. Finite element analysis of the stress distribution during quasi-static indentation suggests that one of the possible mechanism's contribution to material removal is a fatigue-like tensile–compression cyclic loading.

1. Introduction

The removal of material from surfaces in erosive environments can progress by several mechanisms which depend on the angle of impingement and velocity and shape of the erodent particles [1]. For oblique incidence, material loss is mainly the result of cutting and ploughing [2, 3]. For erosion by particles at normal incidence, mechanisms such as extrusion of the surface [4, 5], delamination [6] and fatigue have been proposed [7]. It is evident that the deformation and work hardening [8] that precede the detachment of material in ductile metals is of major importance in altering the surface layers before steady state material removal.

To analyse the fundamental aspects of erosion at normal incidence, experiments based on repeated impacts (up to 10^7) in the same spot on a copper surface, along with *in situ* measurements of material changes were developed. In addition, analyses including finite element calculations for an elastic–plastic work hardening material were developed and conducted. Some of the experimental results are found in works by Iturbe *et al.* [8–10].

The research results presented in this paper are based on the analysis of energy dissipation during the impact. Experiments show that most of the energy expended in each impact belongs to one of three categories, (a) elastic, (b) plastic, and (c) anelastic. The elastic energy is manifested by the portion of the deformation that recovers in the rebound. A measure of the elastic recovery is given by the coefficient of restitution which is the ratio of the square root of the rebound energy to impact energy. The plastic energy loss is associated with the work expended in forming the permanent crater. And finally, the anelastic phenomena occur by energy loss mechanisms such as bowing of dislocations, stress-induced redistribution of point defects, and motion of low-angle boundaries [11]. The anelastic energy loss can occur during both the elastic and plastic deformation. These anelastic mechanisms are significant phenomena, in spite of the amount of plastic deformation [8]. Even in highly elastic impact encounters, the coefficient of restitution is never unity [12]. Much of the energy dissipated is by anelastic processes.

The experimental methods used were described in previous papers [8–10]. They are based upon impacting one point on the specimen with a spherical indenter and repeatedly measuring the time, depth and energy associated with the number of impacts. These experiments demonstrate the significance that work hardening, material

0022–2461/85 $03.00 + .12

flow, nucleation and growth of cracks parallel to the surface have in relation to the flaking and removal of surface layers.

2. Experiments

Annealed copper single crystals and polycrystals were impacted repeatedly at normal incidence on the same point by a single indenter. The spherical surface indenter, a 1.5 mm steel ball attached to a steel rod (to adjust the mass and for design of a mechanically cycling apparatus), is dropped from a fixed distance and accelerated by gravity. After each impact an electromagnet returns the rod to its initial position. By this method, large numbers of impacts can be performed automatically. The record of an impact was made by measuring the instantaneous position of the indenter with a linear variable differential transformer and displaying it in a digital oscilloscope as a function of time, $z(t)$.

Impact and rebound velocities, v_0 and v_r, were obtained as the derivative of the position function with respect to time, $v = dz/dt$, at the time of contact and of separation. The coefficient of restitution, defined as $e = v_r/v_0$, was calculated from the impact and rebound velocities. The depth of the indentation was measured using an optical microscope, and surface and subsurface deformation were analysed by scanning electron microscopy (SEM). The microstructure of the impacted area was studied by transmission electron microscopy (TEM). Impact velocities were varied from 0.15 to 0.65 m sec^{-1}, whereas the indenter mass was adjustable from 100 to 150 g.

3. Energy relationships

Let W_0 be the impact energy, dependent upon the velocity of impact v_0 as given by the expression for the kinetic energy $W_0 = (1/2)mv_0^2$. If the fraction of energy used in plastic deformation is W_p, the elastic energy is W_e, and the anelastic energy is W_a, the following relation holds for the ith impact

$$W_0 = W_p^i + W_e^i + W_a^i \qquad (1)$$

Since the coefficient of restitution, e^i is given by v_r^i/v_0, where v_r^i is the rebound velocity for the ith impact, then the elastic energy can be expressed as

$$W_e^i = W_0 (e^i)^2 \qquad (2)$$

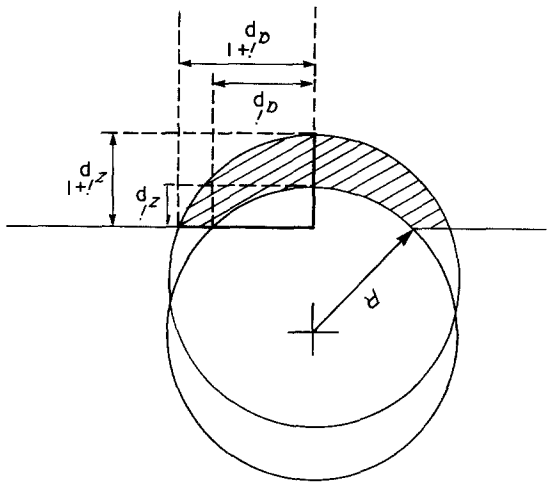

Figure 1 Indenter at maximum penetration for two consecutive impacts, i and $i + 1$.

To obtain an expression for the plastic energy, consider the dimensions of the crater created by the impact as illustrated in Fig. 1, where R is the radius of the indenter, a_p^i is the contact radius, and z_p^i is the depth of the indentation for the ith impact. In the subsequent impact at the same point, the contact radius enlarges to a_p^{i+1}, the plastic deformation boundary advances from z_p^i to z_p^{i+1}, and the plastic work is described in terms of the change in volume from V_p^i to V_p^{i+1} under a stress P^i

$$W_p^i = \int_{V_p^i}^{V_p^{i+1}} p^i \mathrm{d}V_p \qquad (3)$$

The volume of the cap with radius a_p^i in Fig. 1 is

$$V_p^i = (\pi/3)\,(z_p^i)^2\,(3R - z_p^i), \qquad (4)$$

and by solving Equation 3, the plastic energy is

$$W_p^i = P\pi[R(z_p^{i+1} - z_p^i)^2 - (1/3)\,(z_p^{i+1} - z_p^i)^3] \qquad (5)$$

In replacing W_e^i and W_p^i in Equation 1, the anelastic energy can be written as

$$W_a^i = W_0[1 - (e^i)^2] - P\,\pi[R(z_p^{i+1} - z_p^i)^2\,(z_p^{i+1} - z_p^i)^3] \qquad (6)$$

The plastic energy can also be expressed in terms of the impact force F^i

$$W_p^i = \int_{z^i}^{z^{i+1}} F^i \mathrm{d}z_p \qquad (7)$$

If the load is assumed to be constant during impact, equal to an average value of $\bar{F}$, and if the

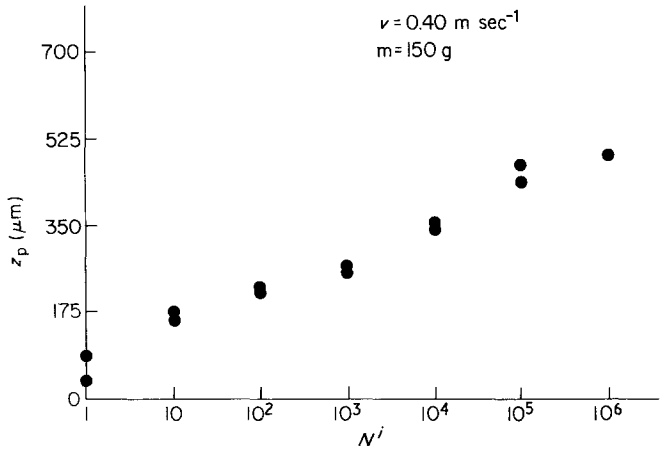

Figure 2 Depth of indentation as a function of number of impacts. Data from two separate experiments are shown.

displacement of the surface is taken to be the change in depth z_p^i from impact i to $i + 1$, an approximate expression for the plastic work is

$$W_p^i = \bar{F}^i \Delta z_p^i \tag{8}$$

4. Experimental results

Impact loading produces a permanent indentation with a well defined edge and a slight "sinking-in" [13] adjacent to the edge in the copper specimens. The depth of the indentations increased after successive impacts. Fig. 2 shows a plot of depth as a function of number of impacts N^i for an impact velocity of $0.40\,\mathrm{m\,sec^{-1}}$. The points in Fig. 2 increase approximately $70\,\mu\mathrm{m}$ per decade, a result that indicates that equivalent penetration is associated with larger numbers of impacts for high N^i, and also that plastic deformation does not reach zero for N^i up to 10^6.

The coefficient of restitution, however, does not approach unity even for very large numbers of impacts, but instead approaches a value of less than 0.8. This effect is shown in Fig. 3. Note the rapid rise during the first ten impacts and the tendency to a horizontal line that extends past 100 impacts.

Fig. 4 shows four traces representing the displacement of the base of the crater surface as a function of time for impacts number 1, 3, 5 and 50, respectively. The traces are arranged such that at the beginning of the impact ($t = 0$), the

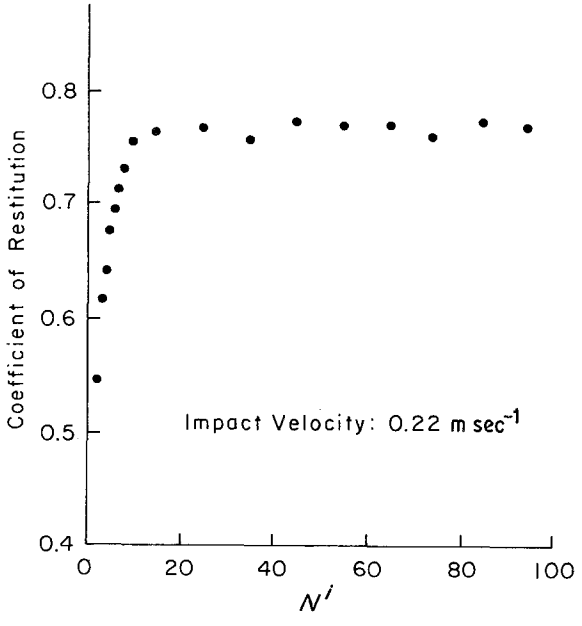

Figure 3 Coefficient of restitution as a function of number of impacts.

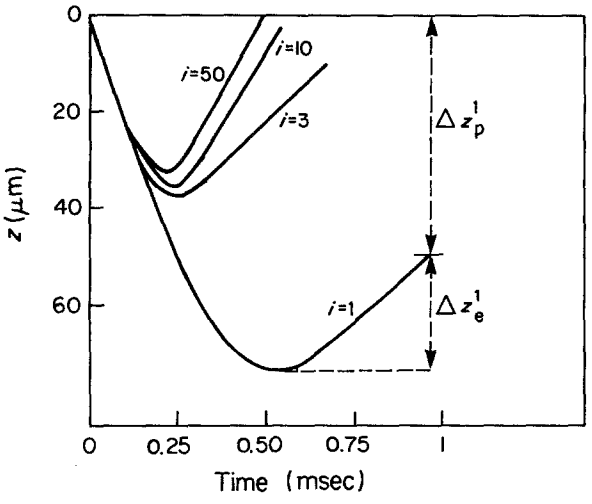

Figure 4 Change in depth of the surface as a function of time during impacts 1, 3, 10 and 50. Impact velocity 0.25 m sec^{-1}.

initial position for each impact coincides at $z^0 = 0$. The traces represent depth changes as a function of time. The end of each trace shows the plastic displacement left at the end of each impact Δz_p^i. The difference between the maximum depth and the final depth is the elastic recovery, Δz_e^i. The distances Δz_p^i and Δz_e^i are shown for simplicity only for impact 1. It can be seen in Fig. 4 that due to the increases in yield stress from work hardening, the duration of the impact and the amount of plastic deformation decrease with each successive impact. The elastic recovery, however, increases with the number of impacts.

The force during the impact is proportional to the second derivative of $z(t)$, thus

$$F = m[\mathrm{d}^2 z(t)/\mathrm{d}t^2] \quad (9)$$

By a numerical analysis of the shape of traces such as those shown in Fig. 4 the force was determined at the point of maximum penetration. This maximum force, $F_{\max}^i$, as a function of the number of impacts is described by

$$F_{\max}^i = 300[1.04 - 0.78\,(N_i)^{-0.37}] \text{ (Newtons)} \quad (10)$$

The plot of Equation 10 is shown in Fig. 5. The maximum force initially increases rapidly and then levels off to a value of about 270 N after about 90 impacts.

From the values of impact and rebound velocities, the fraction of elastic energy in each impact was calculated according to Equation 2. To obtain the values for the plastic work the

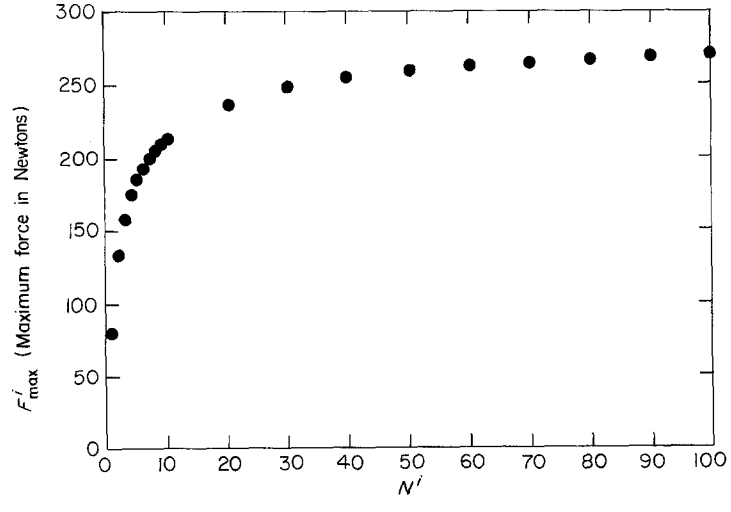

Figure 5 Maximum force as a function of number of impacts. Impact velocity 0.25 m sec^{-1}.

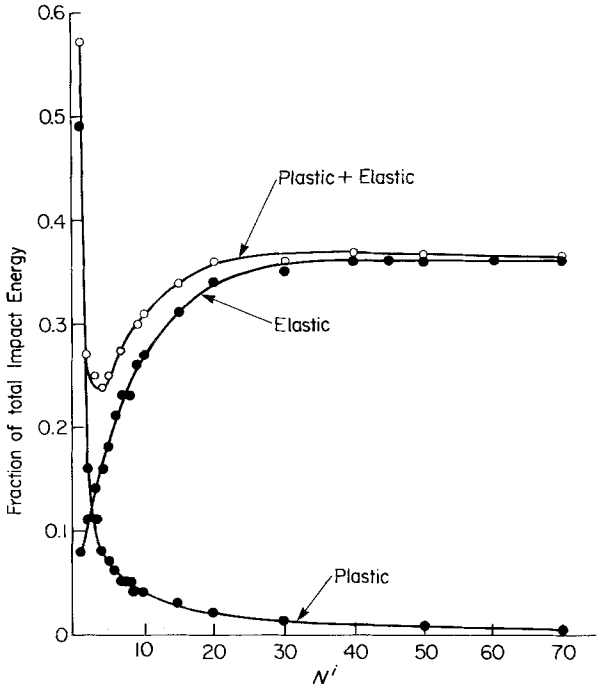

Figure 6 Energy distribution as a function of number of impacts.

value of the average force is needed. An approximation for F was obtained by expressing the elastic work by

$$W_e^i = \bar{F}^i \Delta z_e^i \quad (11)$$

From the coefficient of restitution, $\bar{F}^i$ is calculated. It was found that $\bar{F}^i$ can be approximated by

$$\bar{F}^i = F_{max}^i/3. \quad (12)$$

Using $\bar{F}^i$ from Equation 12 and Δz_p^i from Fig. 4, the plastic work was calculated according to Equation 8. Fig. 6 shows curves representing the fractions of elastic work and plastic work. The difference between the sum of the elastic plus plastic work and unity is the fraction of energy attributed to anelastic behaviour. Data have shown that, after work hardening has become saturated and the amount of energy loss in plasticity is very small, approximately 50% of the total energy is consumed by anelastic processes.

5. Dislocation arrangements

To study the microstructure associated with the impacts, thin foils from approximately 50 μm below the surface were analysed by transmission electron microscopy. Fig. 7 shows the early development of a dislocation cell structure just after ten impacts. The cell walls, not well formed, contain dislocation segments and are jogged at average distances of about 0.05 μm. This figure shows many dislocation segments originating from the tangled dislocation configurations; this observation indicates relatively

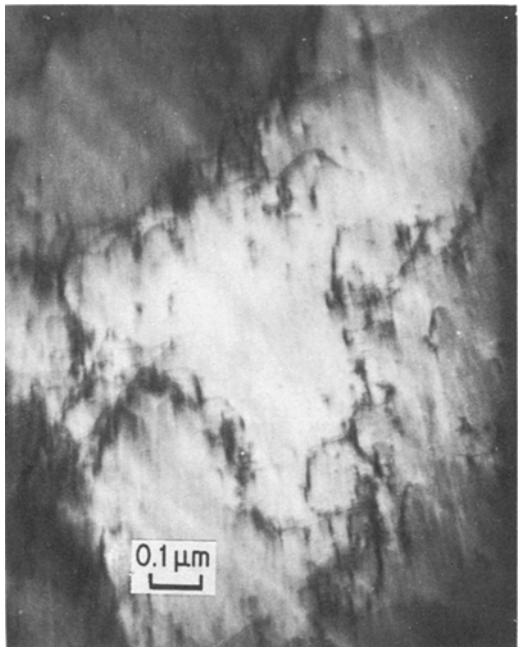

Figure 7 Dislocation structure approximately 50 μm below the surface after ten impacts.

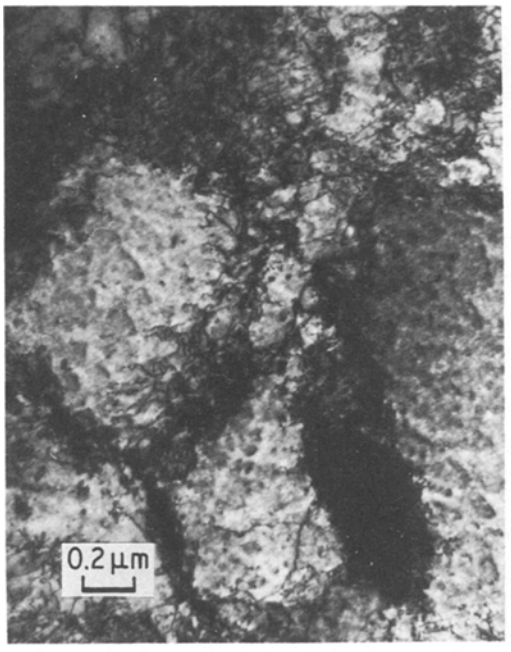

Figure 8 Dislocation structure approximately 50 μm below the surface after 10^4 impacts.

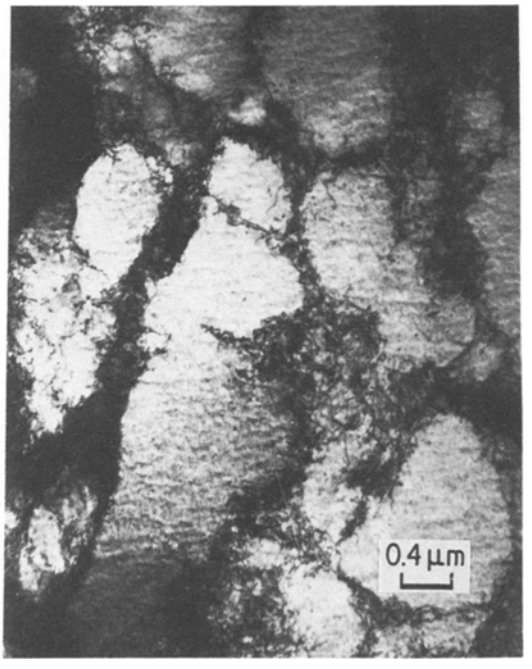

Figure 9 Dislocation structure approximately 50 μm below the surface after 10^4 impacts.

easy sources of dislocation multiplication. In addition, prismatic dislocation loops of a diameter of about 0.01 μm are seen in the clear areas in the cells.

After 10^4 impacts, the cells are better defined and the dislocation and tangle-free areas contain approximately the same density of dislocation loops as in the situation noted for ten impacts (see Figs. 8 and 9). If a comparison is made between the present work and dislocation configurations characteristic of fatigued materials [14], it is concluded that repeated impacts produce dislocation arrangements similar to the cell structure found in copper fatigued at relatively high amplitude.

Thus, two significant dislocation arrangements are evident: (1) the cell structure appears to be similar to that seen in cyclically fatigued copper; and (2) prismatic dislocation loops resemble those observed in quenched copper, in which supersaturation of vacancies are produced.

The experimental data were obtained from a relatively large spherical indenter which impacted the same spot on a surface a predetermined number of times, a process much like a cyclic fatigue. It is useful to compare the present TEM results with those from different experimental conditions such as erosion by a stream of particles reported in the literature [15]. The stress, P, associated with each impact can be approximated by $P = 2mv/ts$, where t is the duration of the impact and s is the average cross section of the impacting particles. An approximation for the time of impact for plastic collisions from Tabor [13] is $0.5\pi(m/2\sigma_0 r)^{1/2}$, with σ_0 being the yield stress for the impacted material and r the radius of the impacting particle. The pressure can thus be expressed as proportional to

$$P \propto \frac{(\sigma_0 m)^{1/2} v}{r^{3/2}} \tag{13}$$

From Expression 13 it follows that the stress developed by the particles in the stream [15], of average mass 5×10^{-7} g, average radius 50 μm, and velocity, 60 m sec^{-1}, is about three times larger than the average stress developed by each single impact in the present experiments. The local stress in the surface layer in contact can be even larger due to the smaller radii of portions of the irregularly shaped particles. It is estimated from the data reported by Ives and Ruff [15] that each area of 25 μm^2 in the target is struck about 50 times with erosive particles. In the experiments

carried out in the present investigation, however, the number of impacts ranged from 1 to 10^7. In the particle stream experiment, TEM showed a high density of dislocations extending deep below the surface with a distinct cell structure but without well-defined cell walls. This microstructure could be characterized as a fatigue dislocation arrangement which has not reached a state of saturation [14].

6. Anelastic behaviour

The experimental observations show that the coefficient of restitution and the dislocation cell structure reach a stable state after a small number of impacts. However, the energy expended in elastic and plastic deformation accounts for about half of the total energy available, most of the remaining energy loss is then dependent upon anelastic effects. A major contributor to the anelastic effect is the bowing dislocations under the fluctuating stress field from the impacts. If the average length of the segments of bowed dislocation after 10 impacts is used, 0.1 to 0.5×10^{-6} m, with a dislocation density of $10^{15}\,\mathrm{cm}^{-2}$, a shear stress calculated from the experimental stress level as $\tau = 3.75 \times 10^8\,\mathrm{N\,m}^{-2}$ and the volume involved in an impact in the present experiment as $0.7 \times 10^{-9}\,\mathrm{m}^3$, the energy associated with the bowing of dislocations is 1.6×10^{-3} J. This value compares well with the experimental value of the impact energy. Although calculations have not been made over the entire range of number of impacts, it is reasonable to assume that the anelastic behaviour is dependent upon the dislocations distribution.

7. Crack formation and flaking

As described earlier in this paper, the dislocation configuration reaches a steady state after a small number of impacts. In a manner somewhat similar to the mechanism of dislocation movement in the fatigue process, dislocations appear to shuttle back and forth to the cell walls creating point defects in their wake. Since this activity also occurs in a region a short distance from the surface, where after the repeated impacts tensile residual stresses are also present [16, 17], the stress conditions are conducive to the agglomeration of vacancies into voids. During the subsequent impact which changes the tensile residual stress to a compressive stress, the void is flattened into a disc shape. Vacancies are absorbed by this growing lenticular defect during the repeated impacts and relaxations. These discs are lenticular nuclei and grow by adding vacancies and by reduction of the high residual elastic strain energy at the edge. When continuous cracks reach the surface, small flakes are released, accounting for the loss in material, leading to erosion in ductile metals.

8. Conclusion

The study of the response of a ductile material to repetitive impacts on the same point showed the following points.

1. The impact energy is distributed among plastic, elastic, and anelastic effects.
2. Anelastic effects are significant even at the early stages of work hardening.
3. A dislocation cell structure similar to that found in fatigued materials developed in the subsurface layers. The presence of voids in the dislocation-free areas suggests that dislocations shuttle back and forth from the cell walls. The dislocation movement is one of the anelastic effects of major significance during impacts.
4. Residual stresses may contribute to a fatigue-like tensile–compressive cyclic loading.
5. A possible mechanism for the nucleation of subsurface cracks is the formation of lenticular cracks due to the continued pounding of coalescent voids.

Acknowledgement

This work was supported by the National Science Foundation under Grant no. DMR-800 7282.

References

1. I. FINNIE, A. LEVY and F. H. McFADDEN, "Erosion: Prevention and Useful Applications", ASTM STP 664, edited by W. F. Adler (Americal Society for Testing and Materials, Philadelphia, 1979) pp. 36–58.
2. I. FINNIE, Proceedings 3rd US National Congress of Applied Mechanical Engineering (American Society of Mechanical Engineers, New York, 1958) pp. 527–32.
3. I. M. HUTCHINGS, "Erosion: Prevention and Useful Applications", ASTM STP 664, edited by W. F. Adler (Americal Society for Testing and Materials, Philadelphia, 1979) pp. 59–76.
4. G. L. SHELDON and A. KANHERE, *Wear* **21** (1972) 195.
5. A. K. COUSENS and I. M. HUTCHINGS, *Wear of Materials* **6** (1983) 382.

6. N. SUH, *Wear* **25** (1973) 111.
7. I. FINNIE, *ibid.* **19** (1972) 81.
8. E. B. ITURBE, I. G. GREENFIELD and T. W. CHOU, *J. Mater. Sci.* **15** (1980) 2331.
9. *Idem,* Proceedings of the 5th International Conference on Erosion by Solid and Liquid Impact, Paper No. 30–1 (Cavendish Laboratory, Cambridge, 1979).
10. *Idem, Wear* **74** (1981–82) 123.
11. C. ZENER, "Elasticity and Anelasticity of Metals" (University of Chicago Press, Chicago, 1948).
12. J. P. A. TILLET, *Proc. Phys. Soc. B* **67** (1954) 677.
13. D. TABOR, "The Hardness of Metals" (Oxford University Press, London, 1951) p. 13.
14. M. KLESNIL and P. LUKAS, "Fatigue of Metallic Materials" (Elsevier, Lausanne, 1980) p. 34.
15. L. K. IVES and A. W. RUFF, "Erosion: Prevention and Useful Applications", ASTM STP 664, edited by W. F. Adler (American Society for Testing and Materials, Philadelphia, 1979) pp. 5–35.
16. Y. YOKOUCHI, T. W. CHOU and I. G. GREENFIELD, *Met. Trans. AIME* **14A** (1983) 245.
17. Y. YOKOUCHI, I. G. GREENFIELD, T. W. CHOU and E. I. ITURBE, *Met. Trans. A* **14A** (1983) 2415.

Received 7 August 1984
and accepted 10 January 1985